

# Microwave antennas based on $\text{Ba}_{1-x}\text{Pb}_x\text{Nd}_2\text{Ti}_5\text{O}_{14}$

M. ENE-DOBRE<sup>a</sup>, M. G. BANCIU<sup>b</sup>, L. NEDELICU<sup>b</sup>, G. STOICA<sup>c</sup>, C. BUSUIOC<sup>b,d</sup>, H. V. ALEXANDRU<sup>a</sup>

<sup>a</sup> *University of Bucharest, Faculty of Physics, Magurele 077125, Romania*

<sup>b</sup> *National Institute of Materials Physics, Magurele 077125, Romania*

<sup>c</sup> *ARMTECH S.A., Curtea de Arges 115300, Romania*

<sup>d</sup> *University POLITEHNICA of Bucharest, Faculty of Applied Chemistry and Materials Science, Bucharest 011061, Romania*

The  $\text{Ba}_{1-x}\text{Pb}_x\text{Nd}_2\text{Ti}_5\text{O}_{14}$  ceramic material (BNT) is very attractive for applications at frequencies around few GHz [1]. The temperature coefficient of the resonant frequency  $\tau_f$  decreases from + 70 ppm/°C to – 15 ppm/°C with the Pb content  $x$  increase up to 0.5. The samples with high Pb content exhibit a dielectric constant up to 86.6, but the product  $Q \times f$  is several times lower than for such microwave ceramics as zirconium tin titanate [1-2]. When a product  $Q \times f$  higher than 6000 is required in order to use the BNT materials at high frequencies, then the Pb content can result from the tradeoff between small temperature coefficient  $\tau_f$  and high quality factor  $Q$ . The features of the BNT dielectric resonators lead to the development of miniaturized dielectric resonator antenna (DRA) with improved characteristics. The DRAs of BNT ceramics presented in this paper exhibit an increased bandwidth due to an optimal height over diameter ratio. For an increased gain and shaping of the overall radiation pattern, an array of dielectric resonator antennas is proposed.

(Received July 19, 2011; accepted October 20, 2011)

*Keywords:* Antenna, Microwave, Ba-Pb-Nd-Ti-O

## 1. Introduction

During recent years we see an increase in usage of mobile telecommunication devices that have the capability to support high data transfer rates of packet switched traffic. Either if it's a smartphone, a tablet or a netbook, the need for user mobility without sacrificing high throughput for multimedia content has increased the need of efficient mobile networks, which can supply good coverage in most areas of a country [3], keeping the users connected to the Internet not only in metropolitan areas, but also in the countryside, the mountains or on sea (mobile networks which use satellite connectivity between the Base Transceiver Stations and Base Station Controller or using powerful point to point links between the land and a fixed point in the sea, for example an oil platform, which has the base station at the end of the microwave link).

The next step in mobile communications is LTE, or long term evolution networks, this is a level 3.95 network, not yet 4G called IMT-A (International Mobile Telecommunications Advanced), but it will prepare the "scene" for it. LTE has evolved from both mobile (HSDPA+) and IEEE/IP standards (802.16 and WiMAX), being developed by 3GPP (3rd Generation Partnership Project) with the help of IETF (Internet Engineering Task Force).

The LTE sets, for mobile communications, a speed of at least 100 Mbit/s downlink and 50 Mbit/s uplink [4]. For this to be achieved a different type of access is used, instead of CDMA, TDMA and WCDMA now it's implemented OFDMA. Orthogonal FDM's spread spectrum technique distributes the data over a large number of carriers that are spaced apart at precise

frequencies. This spacing provides the "orthogonality" in this technique which prevents the demodulators from seeing frequencies other than their own. MIMO (multiple input multiple output antennas – data is sent in multiple streams by multiple antennas to multiple antennas – takes advantage also on multipath) is also a new technique of improving data throughput between mobile equipment and base station [5].

All of this is not possible without antennas, which have good characteristics regardless of temperature, and offer a good signal level for reception/transmission with low power consumption. For this to be achieved, new types of materials are used, special ceramics that are normally used in the microwave systems for energy storage, but with proper excitation and without screening they can become very good electromagnetic radiators [6].

Important low loss dielectric material systems such as perovskites, tungsten bronze type materials, materials in BaO–TiO<sub>2</sub> system, (Zr,Sn)TiO<sub>4</sub>, alumina, rutile, A<sub>n</sub>B<sub>(n-1)</sub>O<sub>(3n)</sub> type materials, LTCC have found applications in this area [7].

Studies were concentrated on dielectric resonator antennas based on Barium Neodymium Titanate as possible materials suitable for antenna applications.

Dielectric ceramics with low-loss, high electric permittivity and enhanced temperature stability are good candidates for microwave applications, from filters and resonators, to substrates and antennas.

The dielectric resonator antennas provide performances superior to other compact antennas as microstrip patch antennas [8], which may exhibit a narrow impedance bandwidth and a reduced efficiency due to the conductive losses in the patch and to the losses due to the

excitation of the surface waves. Although designed for the same frequency, microstrip and dielectric resonator antennas show similar co-polar radiation patterns [6], the DRA exhibits 10 times larger bandwidth, and higher antenna efficiency and a 1 dB higher gain [6].

## 2. Preparation and characterization of BNT resonators

The  $Ba_{1-x}Pb_xNd_2Ti_5O_{14}$  samples based on  $BaO-PbO-Nd_2O_3-TiO_2$  system were prepared by the solid-state reaction technique.

Reagent-grade oxides and salts ( $TiO_2$ ,  $Nd_2O_3$ ,  $Pb_3O_4$ ,  $NiO$ ,  $ZnO$ ,  $BaCO_3$ ) were used as raw materials. They were ball-milled in water for two hours and after that, were calcined at 1200 °C. The resulted powder was crushed and milled again for 2 hours. Mixing was carried out for 2 hours in an agate mortar with agate balls. The mixture was pressed into pellets, which were sintered at temperatures between 1230 °C and 1260 °C for 2 hours. In order to obtain high densities at low sintering temperatures, 0.2 wt % NiO was added for some samples. The NiO sintering addition acts as a grain-growth inhibitor

improving the quality factor  $Q_o$  in microwave domain [1]. The sintered ceramics were polished in order to remove the surface layer and to obtain parallel surfaces for a good control of the resonant frequency.

For  $x = 0$ , the X-ray diffraction patterns show diffraction lines of the dominant phase  $BaNd_2Ti_5O_{14}$  which exhibit orthorhombic structure and few peaks, which are associated to  $BaTi_4O_9$ . Investigated by scanning electron microscopy, the BNT ceramics show polyhedral well formed grains. With the increase of Pb content, the bulk density increases and the grain size increases from 1 to 8  $\mu m$ .

## 3. Microwave dielectric characterization

The dielectric parameters of the BNT material were investigated in microwaves range by using the Hakki-Coleman method, which analyses the resonance modes of the cylindrical resonator [9]. The electromagnetic modes found in a cylindrical dielectric resonator are shown in Fig. 1.

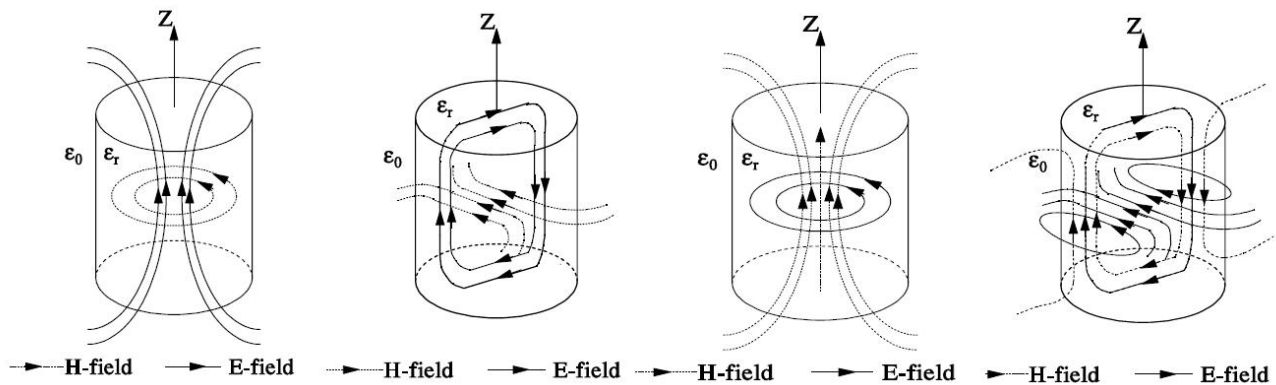


Fig. 1. Sketch for the field distributions of the  $TM_{010}$ ,  $HEM_{11}$ ,  $TE_{01}$ ,  $HEM_{12}$  electromagnetic modes of a cylindrical dielectric resonator [12].

The microwave measurements on  $BaNd_2Ti_5O_{14}$  samples, which do not contain Pb, show an increase of the dielectric constant with the increase in the sintering temperature, the quality factor exhibits a maximum value for the samples sintered at 1250 °C for 2 hours.

For an  $x = 0.33$  Pb content, the dielectric constant increases with the increase of the sintering temperature.

The temperature coefficient  $\tau_f$  takes slightly smaller values as in the case of  $BaNd_2Ti_5O_{14}$ . The highest values of the dielectric constant about 87 were achieved for  $Ba_{0.5}Pb_{0.5}Nd_2Ti_5O_{14}$  samples [10].

The dielectric constant somewhat increases with the sintering temperature and in microwave range can be correlated with the bulk density: both parameters exhibit the highest values for  $x = 0.5$  and they both increase with the increase in sintering temperature.

Furthermore, the lowest value of the temperature coefficient  $|\tau_f| < 15$  ppm/°C was achieved for the  $Ba_{0.5}Pb_{0.5}Nd_2Ti_5O_{14}$  samples [11]. However, the quality factor, which practically does not depend on the sintering temperature, is smaller as in the previous cases for  $x = 0$  or  $x = 0.33$ .

## 4. Dielectric resonator antenna (DRA)

When a dielectric resonator is not entirely enclosed by a conductive boundary, it can radiate, and so it becomes an antenna. Dielectric resonator antennas (DRA) have been exploited in the past at high frequencies (microwave and millimeter-wave range) due to their particular advantages over their metal structure counterparts, such as high efficiency, small size and a simple feeding arrangement

[6]. Because of these advantages, an implementation at cellular frequencies has been explored more recently. One of the main drawbacks of most of the reported designs, however, is the relatively large size of the resonator necessary to achieve an efficient antenna at these frequencies.

To obtain a reasonably sized antenna for such bands, a very high dielectric constant is required, which in turn may lead to an unacceptable reduction in bandwidth. The increase of the dielectric constant affects directly the quality factor ( $Q$ ) of the resonator; in fact  $Q$  increases as  $\epsilon_r^{3/2}$  [12] which results in very narrow band behavior.

The resonant frequency and  $Q$ -factor for the first few modes of the cylindrical resonator are given by the following equations [13]:

TE<sub>01δ</sub> Mode:

$$f_o = \frac{2.921c\epsilon_r^{-0.465}}{2\pi A} \left[ 0.691 + 0.319 \left( \frac{A}{2H} \right) - 0.035 \left( \frac{A}{2H} \right)^2 \right] \quad (1)$$

$$Q = 0.012\epsilon_r^{1.2076} \left[ 5.270 \left( \frac{A}{2H} \right) + 1106.188 \left( \frac{A}{2H} \right)^{0.625} e^{-1.0272 \left( \frac{A}{2H} \right)} \right] \quad (2)$$

HEM<sub>11δ</sub> Mode:

$$f_o = \frac{2.735c\epsilon_r^{-0.436}}{2\pi A} \left[ 0.543 + 0.589 \left( \frac{A}{2H} \right) - 0.050 \left( \frac{A}{2H} \right)^2 \right] \quad (3)$$

$$Q = 0.013\epsilon_r^{1.202} \left[ 2.135 \left( \frac{A}{2H} \right) + 228.043 \left( \frac{A}{2H} \right)^{-2.046} e^{+0.111 \left( \frac{A}{2H} \right)^2} \right] \quad (4)$$

TM<sub>01δ</sub> Mode:

$$f_o = \frac{2.933c\epsilon_r^{-0.468}}{2\pi A} \left\{ 1 - \left[ 0.075 - 0.05 \left( \frac{A}{2H} \right) \right] \frac{\epsilon_r - 10}{28} \right\} \cdot \left\{ 1.048 + 0.377 \left( \frac{A}{2H} \right) - 0.071 \left( \frac{A}{2H} \right)^2 \right\} \quad (5)$$

$$Q = 0.009\epsilon_r^{0.888} e^{0.040\epsilon_r} \left\{ 1 - \left[ 0.3 - 0.2 \left( \frac{A}{2H} \right) \right] \frac{38 - \epsilon_r}{28} \right\} \cdot \left\{ 9.498 \left( \frac{A}{2H} \right) + 2058.33 \left( \frac{A}{2H} \right)^{4.322} e^{-3.50 \left( \frac{A}{2H} \right)} \right\} \quad (6)$$

where  $A$  is the radius and  $H$  is the height of the DRA when mounted on a ground plane. The bandwidth ( $BW$ ) of the DRA is related to the  $Q$ -factor by:

$$BW = \frac{s-1}{Q\sqrt{s}} \cdot 100\% \quad (7)$$

where  $s$  is the desired VSWR at the input port of the DRA.

From the preceding equations for the  $Q$ -factor, it is evident that a lower  $Q$ -factor (and thus larger bandwidth) occurs for smaller values of the dielectric constant. In theory, a DRA with a dielectric constant of one would have the lowest  $Q$ -factor and therefore the widest bandwidth. In practice, however, there is a lower limit on the value of the dielectric constant required to contain the fields within the DRA in order to resonate. It is instructive to look at the typical bandwidth achievable by DRAs of rectangular and cylindrical shapes of low dielectric permittivity [14]. A considerable degree of control over bandwidth is possible by adjusting the aspect ratio of the DRAs. In general, a wider range is achievable for the rectangular DRAs than for the cylindrical DRAs. Also, low profile rectangular DRAs appear to offer the widest bandwidth for a given volume. It is interesting to note that the bandwidth does not increase monotonically with the DRA volume. As the DRA volume increases, the bandwidth initially decreases until it reaches a minimum value, and then increases with volume [15].

Full wave analysis of the antenna configurations were performed using commercially available software [16]. Extensive simulations were carried out using the software in order to obtain optimal design parameters for the antenna.

Knowing the resonance mode, one can predict the far field radiation when utilizing them as antennas, the dielectric resonator excited in TE<sub>01δ</sub> radiates as a short magnetic dipole oriented along its axis, in the TM<sub>01δ</sub> mode, DR radiates as a short electric dipole and in the HE<sub>11δ</sub> mode, the DR resonates as a horizontal magnetic dipole.

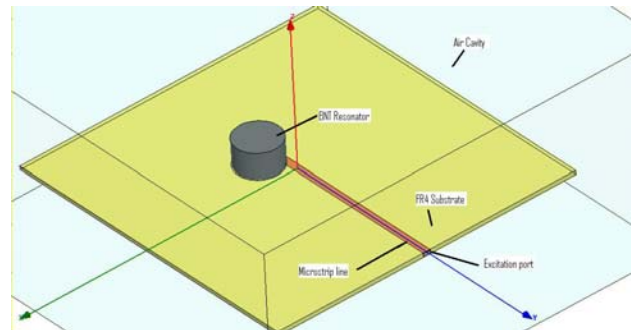


Fig. 2. Geometry of the dielectric resonator antenna.

The dielectric resonator antenna shown in figure 2 is based on a dielectric resonator made from Ba<sub>1-x</sub>Pb<sub>x</sub>Nd<sub>2</sub>Ti<sub>5</sub>O<sub>14</sub> ceramics. The resonator has the permittivity  $\epsilon_r = 58.3$  and a dielectric loss tangent  $\tan\delta = 4.8 \cdot 10^{-4}$ , diameter of 16.95 mm, and height of 10 mm. The resonator is placed on a FR4 epoxy substrate with  $\epsilon_r = 4.4$  and a dielectric loss tangent  $\tan\delta = 2 \cdot 10^{-2}$ . The excitation of the resonator is achieved with the help of a microstrip line with an impedance of 50  $\Omega$ .

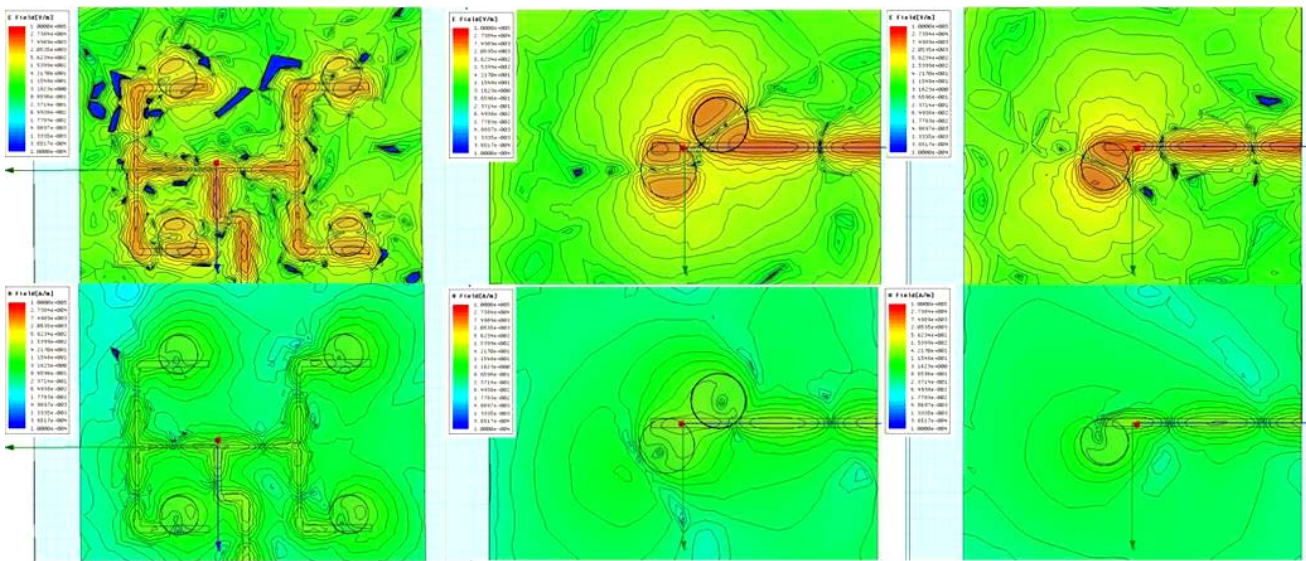


Fig. 3. Field plots for different DRA configurations excited in  $HEM_{11\delta}$  mode: magnetic field (lower row), electric field (upper row).

From figure 3 it can be observed the coupling intensity between the resonators and the microstrip line, and the electromagnetic modes that are present in the resonator at certain frequencies, here around 2.4 GHz.

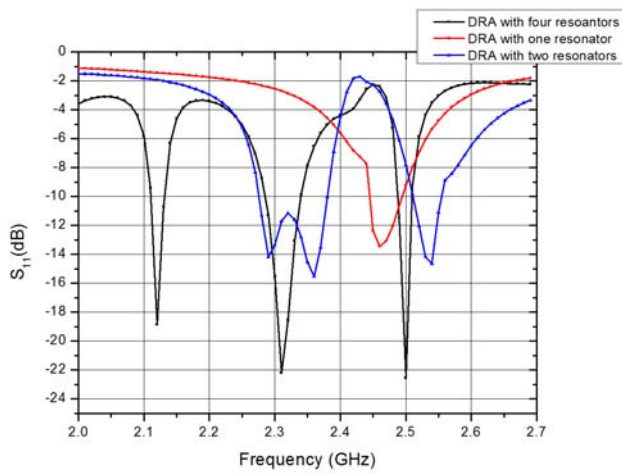


Fig. 4.  $S_{11}$  parameter for different antenna configurations.

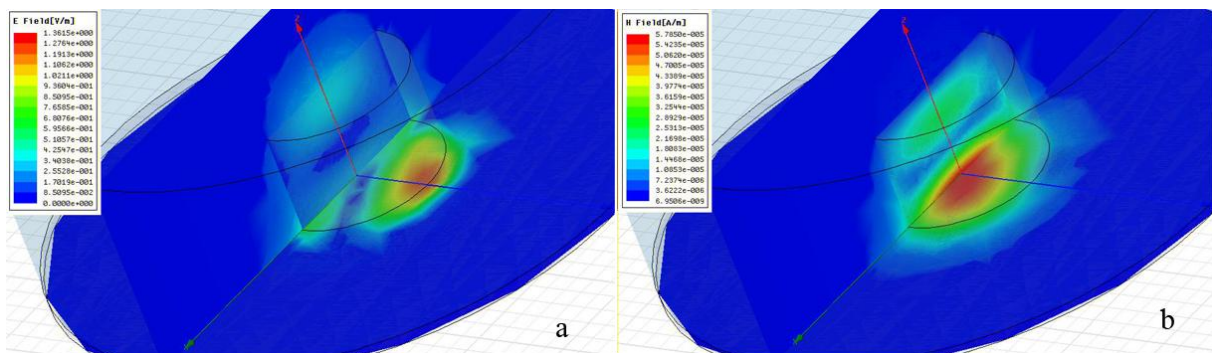


Fig. 5. The field distribution for  $TE_{01\delta}$  mode at 2.48 GHz of a BNT dielectric resonator: a) electric field, b) magnetic field.

For two resonators we see an increase in bandwidth from 50 MHz for one resonator to 100 MHz for two resonators, lower resonating frequency provides lower bandwidth available compared to ZST resonators. Also an additional resonance for 2 resonator configuration could provide a FDD configuration (downlink/uplink frequency allocation), the lower bandwidth can be allocated to uplink frequency which usually has a lower data rate transfer.

The bandwidth available is strictly related on how the resonators are situated in respect to the microstrip line or feeding network (symmetric or asymmetric), thus the coupling between the line and the resonators, but also is influenced by the coupling between the resonators. We can observe this looking at the four resonator array. Although the bandwidth should be greater, we see that the resonances of the resonators uncoupled don't create a continuous bandwidth, but a split band of frequencies. This can be avoided by obtaining a good coupling between the resonators and between them and the transmission line.

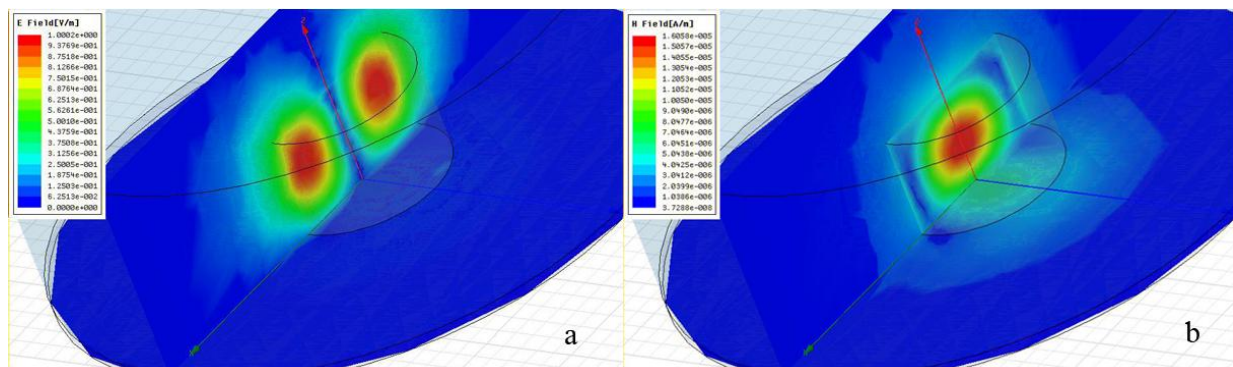


Fig. 6. The field distribution for  $HEM_{11\delta}$  mode at 2.49 GHz of a BNT dielectric resonator: a) electric field, b) magnetic field.

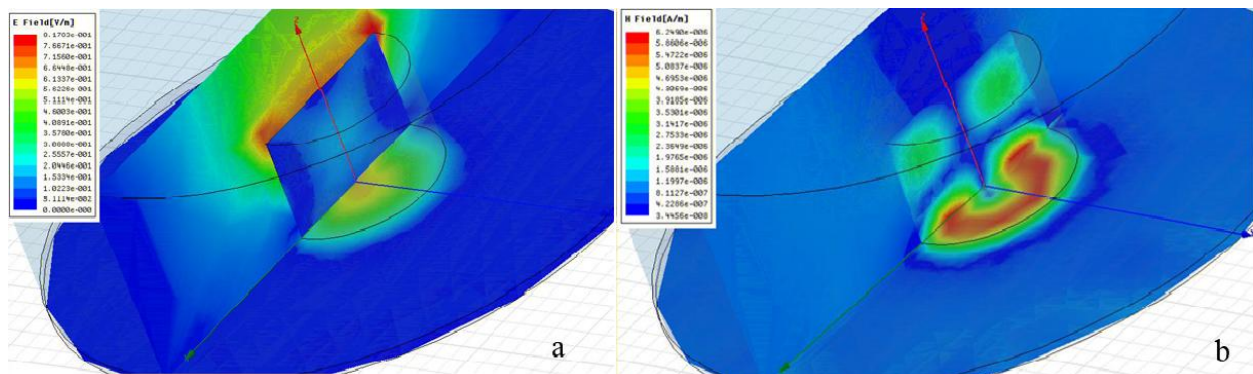


Fig. 7. The field distribution for  $TM_{01\delta}$  mode at 2.79 GHz of a BNT dielectric resonator: a) electric field, b) magnetic field.

In Figs. 5, 6 and 7 we can see the electric and magnetic field distribution for the first three modes of the cylindrical dielectric resonator described previously. From equations (1), (3) and (5) we obtain for  $TE_{01\delta}$  mode a resonant frequency of 2.04 GHz compared with the data computed by HFSS, for  $HEM_{11\delta}$  mode at 2.05 GHz and for  $TM_{01\delta}$  mode at 2.83 GHz.

## 5. Antenna array with four DRA

The proposed antenna configuration is composed from four BNT resonators placed on a FR4 epoxy substrate. The resonators are excited by means of a microstrip feeding network. The distance between the resonators is  $\lambda_0/2$ , where  $\lambda_0$  is the free space wavelength. Using strip coupling, the resonator is usually positioned at a distance of  $\lambda_g/4$  away from the open end of the microstrip line, where  $\lambda_g$  is the guided wavelength of the microstrip guiding structure. The width and length of the slot need to be appropriately chosen so that good matching to a 50  $\Omega$  microstrip line is obtained for each DRA element.

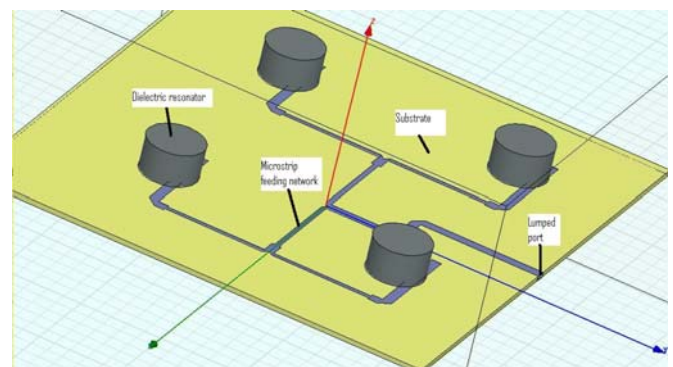


Fig. 8. Geometry of the microstrip fed antenna array with 4 elements.

In Fig. 9 it is shown the radiation pattern of the dielectric resonator antenna based on a single BNT resonator. The antenna is showing a maximum gain of 6 dB for the main lobe. Due to the characteristics of the  $HE_{11\delta}$  mode, the radiation pattern is similar to the pattern due of a magnetic dipole placed horizontally, along the microstrip feeding line. The width of the lobe is about  $110^\circ$  (for  $\phi = 90^\circ$ ) and  $100^\circ$  (for  $\phi = 0^\circ$ ).

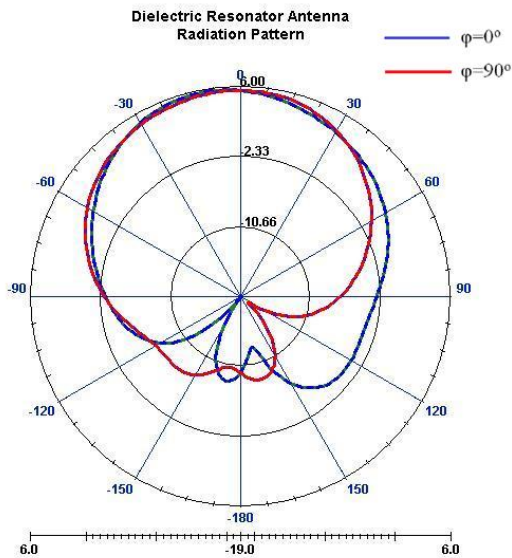


Fig. 9. Antenna pattern of a single BNT DR antenna.

There is an increase in gain for the antenna with four elements, also the pattern becomes more concentrated. The gain is lower compared to the ZST DRA [2]. In this case, the main lobe width is  $70^\circ$  (for  $\phi = 90^\circ$ ) and  $65^\circ$  (for  $\phi = 0^\circ$ ). Compared with the antenna based on zirconium tin titanate, the barium neodymium titanate antenna exhibits lobes that cover a greater side area but at expense of a lower gain.

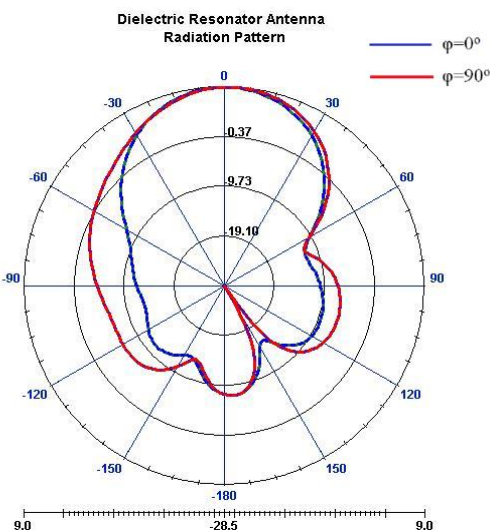


Fig. 10. Antenna radiation pattern of the 4-element antenna array shown in Fig. 8.

## 6. Conclusions

The BNT based DRA can be used in lower frequencies around ISM band, and due to high permittivity gives a high miniaturization of the antenna system. The frequency bandwidth is enhanced by adding an extra dielectric resonator to the structure. High directivity and

gain was achieved by designing a four element antenna array. There is no inherent conductor loss in dielectric resonators, leading to high radiation efficiency of the antenna. BNT based DRAs offer simple coupling schemes to nearly all transmission lines used at microwave and mm-wave frequencies. This makes them suitable for integration into different planar technologies. The coupling between a DRA and the planar transmission line can be easily controlled by varying the position of the DRA with respect to the line. The performance of DRA can therefore be easily optimized experimentally. Each mode of BNT DRA has a unique internal and associated external field distribution. Therefore, different radiation characteristics can be obtained by exciting different modes of a DRA. BNT ceramic resonators are a good choice for high gain, compact antennas with special characteristics that are constant with temperature variation.

## Acknowledgement

The work has been partially supported by the Romanian Ministry of Education and Research, project 12-078/2008.

## References

- [1] A. Ioachim, M. I. Toacsan, M. G. Banciu, L. Nedelcu, C. A. Dutu, G. Stoica. *J. Optoelectron. Adv. Mater.* **9**, 1572 (2007).
- [2] M. Ene-Dobre, M. G. Banciu, L. Nedelcu, A. Ioachim, H.V. Alexandru, *J. Optoelectron. Adv. Mater.* **12**, 1926 (2010).
- [3] Christophe Chevallier, Christopher Brunner, Andrea Garavaglia, Kevin P. Murray, Kenneth R. Baker, "WCDMA (UMTS) Deployment Handbook Planning and Optimization Aspects", John Wiley & Sons 2006.
- [4] \*\*\*, "LTE/SAE system overview", Ericsson Corporation 2010.
- [5] Harri Holma, Antti Toskala, "LTE for UMTS – OFDMA and SC-FDMA Based Radio Access", John Wiley & Sons 2009.
- [6] Aldo Petosa, "Dielectric Resonator Antenna Handbook", Artech House 2007.
- [7] Mailadil T. Sebastian, "Dielectric materials for Wireless communications", Elsevier 2008.
- [8] R. Chair, A. A. Kishk, K. F. Lee, D. Kajfez, *Microwave Journal*, **49**, 90 (2006).
- [9] B. W. Hakki, P. D. Coleman, *IRE Trans. Microwave Theory and Techn.*, **MTT-8**, 402 (1960).
- [10] Nicolaescu Ioan, Ioachim Andrei, Toacsan Irina, Radu Ionut, Banciu Gabriel, Nedelcu Liviu, *WSEAS Transactions On Communications Issue 5, Volume 7*, May 2008.
- [11] A. Ioachim, M. I. Toacsan, M. G. Banciu, L. Nedelcu, H. Alexandru, C. Berbecaru, D. Ghetu, G. Stoica, *Materials Science and Engineering B* **109**, 183 (2004) Elsevier.

- [12] Ahmed A. Kishk, Chapter 4 from “Dielectric resonator antennas”, “Body of Revolution (BOR) – Analysis of Cylindrical Dielectric Resonator Antennas”, Department of Electrical Engineering, University of Mississippi, USA.
- [13] Aldo Petosa, Apisak Ittipiboon, Yahia Antar, Chapter 5 from “Dielectric resonator antennas”, “Broadband Dielectric Resonator Antennas”, Communications Research Centre Canada, Ottawa, Canada.
- [14] M. Saed, R. Yadla, ”Microstrip-Fed Low Profile And Compact Dielectric Resonator Antennas”, Progress In Electromagnetics Research, PIER 56, 151–162, 2006.
- [15] Mihai D. Rotaru, Jan K. Sykulski, IEEE Transactions On Magnetics, **45**(3), March 2009.
- [16] \*\*\*, “HFSS 12 Documentation”, Ansys-Ansoft Corporation, Pittsburgh, USA, 2010.

---

\*Corresponding author: enedobremihai@gmail.com